Transnational University Limburg is a unique collaboration of two universities in two countries: the University of Hasselt and Maastricht University.

UHASSELT
KNOWLEDGE IN ACTION

www.uhasselt.be
Universiteit Hasselt
Campus Hasselt:
Martelarenlaan 42 | 3500 Hasselt
Campus Diepenbeek:
Agoralaan Gebouw D | 3590 Diepenbeek

UHASSELT
KNOWLEDGE IN ACTION

Maastricht University

Faculty of Medicine and Life Sciences
School for Life Sciences
Master of Biomedical Sciences

Master's thesis

One-pot synthesis and processing of strong and tough PEGDMA-based dual network hydrogels for tissue engineering

Anneleen Jacobs

Thesis presented in fulfillment of the requirements for the degree of Master of Biomedical Sciences, specialization Bioelectronics and Nanotechnology

SUPERVISOR :
Prof. dr. Louis PITET

MENTOR :
Mevrouw Mariana ARREGUIN CAMPOS

2023
2024

UHASSELT
KNOWLEDGE IN ACTION

Maastricht University

Faculty of Medicine and Life Sciences
School for Life Sciences
Master of Biomedical Sciences

Master's thesis

One-pot synthesis and processing of strong and tough PEGDMA-based dual network hydrogels for tissue engineering

Anneleen Jacobs

Thesis presented in fulfillment of the requirements for the degree of Master of Biomedical Sciences, specialization Bioelectronics and Nanotechnology

SUPERVISOR :

Prof. dr. Louis PITET

MENTOR :

Mevrouw Mariana ARREGUIN CAMPOS

One-pot synthesis and processing of strong and tough PEGDMA-based dual network hydrogels for tissue engineering

Anneleen Jacobs[1], Mariana Arreguin Campos[1], and Louis Pitet[1]

[1]Advanced functional polymer group, Institute for Materials Research, Universiteit Hasselt, Campus Diepenbeek, Agoralaan Gebouw D - B-3590 Diepenbeek

*Running title: *PEGDMA-based DN hydrogels for tissue engineering*

To whom correspondence should be addressed: prof. dr. Louis Pitet, Tel: +32 (11) 26 83 20; Email: Louis.pitet@uhasselt.be

Keywords: Dual network hydrogel, alginate, gelatine methacrylate, 3D printing, poly(ethylene glycol) dimethacrylate

ABSTRACT

Hydrogels are hydrophilic polymeric materials that have garnered significant interest for biomedical applications due to their tunability and high water retention, which makes them similar to biological tissues. However, traditional single network hydrogels often lack the mechanical strength required for load-bearing applications, restricting their application. To address this, combining different networks has emerged as a promising strategy to enhance the mechanical performance of biomaterials. This study focuses on the synthesis and characterization of dual network PEGDMA-based hydrogels incorporating alginate, alginate methacrylate (AlgMA), and gelatine methacrylate (GelMA). These combinations utilize different crosslinking mechanisms for a one-step synthesis and improved mechanical performance. The biocompatibility of the systems was investigated via the seeding of ATDC5 cells on hydrogels. The system of PEGDMA-SH/alginate demonstrated enhanced toughness under tensile conditions, likely due to the energy dissipation provided by the alginate network. The PEGDMA-SH/AlgMA system exhibited to be a strong network under compression but showed increased brittleness under tensile testing. Meanwhile, the system of PEGDMA-SH/GelMA exhibited increased mechanical strength and brittleness in compression and tensile experiments, respectively. PEGDMA-SH/alginate was selected to demonstrate the possibility of 3D printing a dual network via embedded 3D printing. In summary, the three dual network systems developed in this study showed enhanced mechanical properties compared to the PEGDMA-SH single network hydrogel, showcasing good biocompatibility.

INTRODUCTION

The field of tissue engineering aims to restore the functionality of diseased tissue through an interdisciplinary approach that combines cells, biomaterials, and signaling molecules (Fig. 1) (1, 2, 3). Successfully integrating these elements and restoring the diseased tissue requires understanding the innate tissue structure and the signals it receives (1, 4). Ideally, one would aim to precisely replicate the extracellular matrix (ECM) of the diseased tissue. However, this is challenging due to the complexities of the native tissue, including intricate signaling pathways and dynamics of the structure (1, 5, 6, 7). Scaffolds aim to fulfill various functions, such as providing structural support, facilitating cell adhesion, and carrying cell signals, thereby trying to mimic the ECM as closely as possible (6, 7). Materials used for the fabrication of scaffolds can be polymeric, ceramics, synthetic proteins, and even de-cellularized matrices. (5, 6, 7). Ideally, the created materials can be processed using conventional techniques like freeze-drying or solvent casting or additive manufacturing techniques such as stereolithography or 3D printing to fit the needs of each individual patient optimally (8).

Hydrogels are an important type of biomaterial that has been studied extensively as scaffolds (9). They are hydrophilic 3D networks that can retain up to 1000 times their original weight in water, which makes them similar to biological tissues, biocompatible, and, thus, interesting for biomedical applications (10, 11). The polymers comprising hydrogels can be divided into naturally derived or

synthetically produced (7, 12). Naturally derived polymers, like the ECM components alginate, collagen, fibrin, and silk fibers, are interesting due to their high biocompatibility. However, they show some drawbacks related to their origin, making them prone to batch-to-batch variations and limited in their mechanical properties (7, 9, 12, 13). On the other hand, synthetic polymers, like poly(ethylene glycol) (PEG), poly(lactic acid), and poly(vinyl alcohol), are more reproducible and can easily be tuned for each specific application (7, 12). This class of polymers can be readily functionalized to introduce specific characteristics; for example, introducing methacrylate groups to certain polymers can allow photocrosslinking of the network. Moreover, the chemical composition and the architecture of the final structure can be controlled effortlessly (2, 9, 14, 15). The aforementioned polymers (both natural and synthetic) can be readily used to form hydrogels consisting of a single type of polymer (single network hydrogels) (16). Generally, these materials are soft and elastic, making them ideal for applications such as contact lenses or wound patches. Nevertheless, these hydrogels are mechanically weak, rendering them unsuitable for load-bearing applications, such as restoring bone or cartilage (17, 18). Combining different networks could improve the mechanical properties of the hydrogels, making them suitable for a broader range of applications (16).

PEG is an attractive synthetic polymer for biomedical applications due to its hydrophilic nature, biocompatibility, low immunogenicity, and resistance to protein adsorption (13, 14, 19). Furthermore, it can be easily functionalized to introduce certain properties, such as incorporating acrylates (PEGDA) or methacrylates (PEGDMA) to enable photopolymerization (14, 20, 21). A recent paper by Arreguín-Campos et al. described a system in which linear PEGDMA was combined with a multi-arm PEG-thiol molecule to increase the homogeneity of the system (22). This addition of the multi-arm thiol molecule improved the mechanical properties of the hydrogel compared to the homopolymer network, emphasizing the significance of the architectural composition of the network. Furthermore, they demonstrated the potential for digital light processing of these hydrogels due to the photosensitivity of the methacrylate groups. As a result, this system has shown great potential for advanced, load-bearing applications. Despite its potential, the system lacks a built-in energy dissipation mechanism, meaning that when a crack is created, propagation will happen quickly, leading to fast fracture (23). Combining this system with an additional network could address such limitations while endowing the material with other desired characteristics, such as improving cell adhesion. An example of this has been provided by Ishikawa et al (24). They created a system in which PEG was combined with a self-assembling peptide (RADA16) to incorporate cell adhesive properties. RADA16 will form a β-sheet nanoscale network when it is immersed in an ion-containing buffer solution, while the tetra-PEG network will assemble via chemical crosslinking between maleimide-functionalized PEG (PEG-MA) and sulfhydryl-functionalized PEG (PEG-SH) molecules. By employing this orthogonal crosslinking mechanism, they formed a hydrogel that possessed tough and biocompatible properties

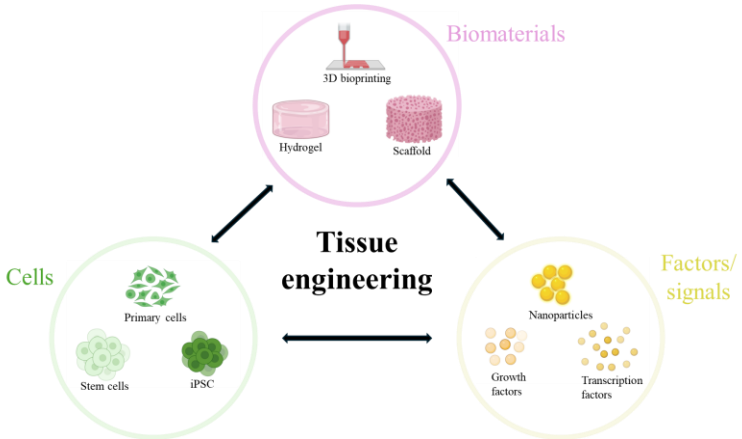

Fig. 1: The three different pillars of tissue engineering.

with increased cell adhesion due to the addition of the peptide. Yuan et al. employed a similar approach by introducing polyurethane (PU) into a PEGDA network (25). Both networks were functionalized with acrylate groups and subsequently crosslinked under UV light. They saw that by introducing the PU into the network, the mechanical properties could be tuned to form softer networks while also facilitating cell adhesion and bioactivity.

Thus, creating double network hydrogels could form an alternative to the aforementioned downsides as they combine two polymer networks to achieve enhanced mechanical properties and introduce other desired characteristics. These were first described by Gong et al., which showed that by combining two networks, the mechanical strength significantly increased (17). Herein, the first network is a rigid, brittle, tightly crosslinked polyelectrolyte, while the second is a loosely crosslinked soft and ductile neutral polymer. Both networks contribute to the final structure, making them mechanically robust and thus ideal for load-bearing applications (17, 26, 27). In a paper by Sun et al., double network hydrogels based on alginate and acrylamide were developed (28). Herein, the first network uses physical crosslinking, while the second employs covalent crosslinking. The ionic bonding of the alginate network introduced an energy dissipation mechanism in which the physical crosslinks could reform after deformation, whereas the acrylamide network remained intact and stabilized the deformation. Though these systems introduced several properties into the hydrogels, the synthesis is often a multi-step process and time-consuming process, which is not ideal for patient-tailored applications (11).

In this study, we synthesize and characterize dual network hydrogels based on the previously reported PEGDMA-3SH system, combined with naturally derived polymers: alginate, alginate methacrylate (AlgMA), and gelatin methacrylate (GelMA). We hypothesize that by introducing an additional network, the mechanical properties can be enhanced. We examine the impact of having interconnected networks by using purely ionically crosslinked alginate and comparing it against AlgMA and GelMA. Additionally, GelMA is used as a means to introduce biological motifs into the system, promoting cell attachment. We make use of methacrylate to enable photopolymerization of the materials, facilitating their processability. The properties of the hydrogels are determined via compression, tensile, and swelling testing. The biocompatibility is evaluated using chondrocytes, the resident cells of joints responsible for bone and cartilage formation. As a proof-of-concept, embedded 3D printing is demonstrated for the processability of the PEGDMA-SH/alginate dual network. Hence, these systems could provide new materials with enhanced mechanical performance for patient-tailored applications in load-bearing tissues like cartilage and bone.

EXPERIMENTAL PROCEDURES

Materials – Glycerol ethoxylate (molar mass 1.0 kg mol^{-1}), 3-mercaptopropionic acid (>99%), methacrylic anhydride (MA, > 94%), sodium alginate (low viscosity), and lithium phenyl-2,4,6-trimethylbenzoylphosphinate (LAP) were obtained from Sigma-Aldrich (Belgium). Toluene (> 99.8%), dichloromethane (DCM, > 99%), diethyl ether (Et_2O, > 99.5%), sodium hydroxide (NaOH, 99%), glucono δ-lactone (GDL, 99%), phosphate-buffered saline (PBS), and Dulbecco's modified Eagle's medium (DMEM) were purchased from Fisher Scientific (Belgium). Sulfuric acid (H_2SO_4, > 95%), sodium bicarbonate ($NaHCO_3$, > 99.8%), magnesium sulfate ($MgSO_4$, 99%), calcium sulfate ($CaSO_4$, > 98%), and calcium carbonate ($CaCO_3$, > 98%) were provided by Acros Organic (Belgium). Poly(ethylene glycol) (PEG, molar mass 10.000 and 20.000 g mol^{-1}) was obtained from Merck KGaA (Germany). Gelatine methacrylate (GelMA) was provided by Polbionica (Poland), and Honeywell (the Netherlands) provided calcium chloride ($CaCl_2$).

3-arm PEG-SH synthesis – Glycerol ethoxylate (10 g, 10 mmol), 3-mercaptopropionic acid (6.5 mL, 74.8 mmol), and toluene (100 mL) were combined in a round bottom flask and heated to 80°C. After adding three drops of H_2SO_4, the mixture was heated until 130°C (reflux) and reacted for 24 hours under Dean-Stark conditions. The solvent was then evaporated under a vacuum, and the resultant oil was dissolved in DCM and washed with saturated $NaHCO_3$ and brine. After drying the solution with $MgSO_4$ and filtration, the solvent was removed in vacuo. This yielded a clear, light-yellow oil, which was further dried overnight under vacuum. ^1H NMR ($CDCl_3$, 400 MHz): δ 4.22-4.25 (qu, $–CH_2OCO–$), 3.46-3.74 (m, $–OCH_2CH_2O–$),

2.72-2.79 (m, $–CH_2SH$), 2.62-2.68 (m, $–OCCH_2–$)1.65 (t, -SH).

Microwave-assisted PEGDMA$_{10kDa}$ synthesis – Poly(ethylene glycol) with a molar weight of 10 kDa (PEG_{10kDa}, 10 g, 1 mmol) was mixed with a five molar excess of MA (0.74 mL, 5 mmol) in an 80 mL vial. The mixture was then placed in a microwave reactor (CEM Discover SP), after which an inert environment was employed. This was left to react for 30 minutes at 130°C with maximal stirring. Afterward, the product was dissolved in DCM and precipitated in cold Et_2O. This was subsequently filtered and redissolved in DCM. Most of the solvent was evaporated before repeating the precipitation and filtration steps. This process was repeated until a total of three precipitations were completed. Finally, the product was dried on a vacuum line, yielding white powder. ^1H NMR ($CDCl_3$, 400 MHz): δ 5.56-6.11 (m, $–CH_2C–$), 4.27-4.30 (t, $–CH_2CH_2OCO–$), 3.48-3.68 (m, $–OCH_2CH2O–$), 1.93 ($–CH_3CH–$).

Alginate purification – Sodium alginate was dissolved for 24h at 4°C in deionized water to achieve a final concentration of 1% (w/v). Subsequently, 0.5% (w/w) active charcoal was added and left to react for another 24h at 4°C. Afterward, the solution was filtered using 1.2 µm, 0.8 µm, 0.45 µm, and 0.2 µm filters to remove the charcoal from the mixture. Finally, the alginate was freeze-dried (Analis Alpha 1-2 LDplus).

Alginate methacrylate synthesis – A 1% solution of purified alginate was prepared, to which two equivalents MA was added. The pH of the mixture was adjusted to 8 with 5M NaOH and closely monitored. The solution was left to react for 23 h at 4°C, after which the product was purified through dialysis (pore size 6-8 kDa) for 72 hours. The water was changed twice a day. ^1H NMR ($CDCl_3$, 400 MHz): δ 5.61-6.11 (m, $–CH_2C–$), 1.69-1.88 (s, $–CH_3–$).

Alginate-PEGDMA-SH hydrogels with CaSO$_4$ – Hydrogels were prepared by first dissolving $PEGDMA_{10kDa}$ (20 wt.%) in water, after which 3-arm PEG-SH and 0.3 wt.% LAP were added. Then, different alginate concentrations (1, 1.5, and 2% wt.%) were incorporated. This was shortly mixed, and $CaSO_4$ (5 and 10 wt.%[1]) was added. This solution was sonicated until the calcium was evenly dispersed. When the mixture was free of bubbles, it was transferred to the desired molds for mechanical and swelling testing. Final structures were obtained by curing the molds for 15 min in a UV crosslinker (Analytik Jena UV) with a wavelength of 254 nm and an intensity of 30 mJ/cm².

PEGDMA-SH/alginate hydrogels with CaCO$_3$ – 15 or 20 wt.% $PEGDMA_{10kDa}$ or $PEGDMA_{20kDa}$ were dissolved in water before 3-arm PEG-SH and 0.3 wt.% LAP were added. Then, alginate was introduced (1 and 2 wt./wt.%) and properly mixed before $CaCO_3$ (10, 30, 45, and 60%) was dispersed in the ultrasonicated bath. Subsequently, GDL (ratio with $CaCO_3$, varying between 1:2 and 1:6.5) was added to crosslink alginate. The solutions were added to the desired molds and placed in a humidifier (85% humidity, 25°C) for 60-90 minutes, after which the molds were cured similarly in the UV crosslinker.

Preparation of PEGDMA-SH/AlgMA hydrogels – AlgMA (1 or 2 wt.%) and 15 wt.% PEGDMA (MW: 10kDa or 20kDa) were dissolved separately and subsequently added together. LAP (0.3 wt.%) and 3-arm PEG-SH were dissolved and added to this mixture. After this, 10 wt.% $CaCO_3$ was incorporated, after which the solution was placed in the ultrasonicated bath for about 8 minutes or until adequately dispersed. GDL (1:2 ratio with $CaCO_3$) was mixed in afterward by vortexing the solution to distribute the particles evenly. The solution was added to the molds and placed in the humidifier for physical crosslinking for 1 hour (85% humidity, 25°C). Finally, the hydrogels were crosslinked under UV light for 15 minutes.

Preparation of PEGDMA-SH/GelMA hydrogels – 3-arm-SH and LAP (0.3 wt.%) were dissolved in water and added to 15 wt.% $PEGDMA_{10\ or\ 20kDa}$. This was left to dissolve, and subsequently, 2 or 5 wt.% GelMA was added. The mixture was shortly ultrasonicated to dissolve the GelMA properly. The solution was transferred to the molds for mechanical testing and placed in the UV curing system for 15 minutes to obtain the final structure.

Mechanical characterization – Compression testing was performed on a Shimadzu AGS-X tensile tester with a load cell of 500 N. The triplicate cylindrical samples were 8 mm in diameter and 3

[1] All Ca^{2+} percentages are relative to alginate.

mm in height. Each test had a preload force of 0.05 N and a 1 mm/min velocity. The maximum strain was set to 90%, and the elastic modulus was calculated between 10 and 20% strain. Cyclic compression was performed similarly, in which the maximum strain increased stepwise from 30 to 90 %, returning to 0% after each cycle.

Tensile testing was performed on the same instrument, using dog-bone-shaped samples (triplicates, 2.15 mm in thickness, 3.55 mm in width, and 18 mm long). A load cell of 500 N and a preload of 0.01 N were employed. Each hydrogel was clamped and elongated at a 5 mm/min speed until breakage. Triplicates of the samples were tested.

Swelling testing - Different compositions of cylindrical hydrogels (triplicates) were prepared for swelling testing. After preparation, the gels were dried overnight in a vacuum oven at 50°C, and their weights were recorded. They were then submerged in water, with regular water changes, recording their weight each time. Once the gels reached equilibrium weight, they were dried again, and their final dry weights were recorded. This allowed for the calculation of the gel fraction (GF) equilibrium water content (ECW), mesh size (ζ), crosslink density (ρ), and swelling factor (SF) (See supplementary information for more details).

Cell studies – Single network hydrogels with $PEGDMA_{10kDa}$-SH with and without arginyl glycyl aspartic acid (RGD) and dual networks with 2% alginate, 1% AlgMA, and 2% GelMA were prepared as described earlier. RGD (1 mM) was added to the alginate and AlgMA samples for cell attachment. The gels were prepared 48 hours before seeding and submerged in PBS to allow swelling. After this, the gels were washed with DMEM, which was removed before seeding ATDC5 cells (15.000 cells/well) on the hydrogels. After 24 hours, the cells were fixed and stained with DAPI and phalloidin. Images were recorded on a Nikon TI-E epifluorescent microscope and processed with ImageJ.

Embedded 3D printing – The processability of these systems was investigated by printing multi-layered structures using the extrusion-based BioX bioprinter (Cellink, Fig. S8a). A solution based on the alginate system was prepared as described previously. Briefly, $PEGDMA_{10kDa}$-SH was dissolved and mixed with 2 wt.% alginate until homogeneous; no calcium was added, as it is provided by the support bath (See SI). These solutions were loaded into printing cartridges, connected to 23G needles for printing, and attached to a pneumatic printhead. After printing two layers, the structure was exposed to UV irradiation (365 nm) for 30 sec before adding additional layers. Post-printing, the structures were left in the support bath for 30 minutes to allow physical crosslinking before the support bath was removed in a warm water bath.

RESULTS AND DISCUSSION

3-arm PEG-SH synthesis – A transesterification under Dean-Stark conditions takes place to add the thiol to the multi-arm PEO molecule (Fig. S1b). Under the influence of the acid, the hydroxy group of the glycerol ethoxylate reacts with the one present in 3-mercaptopropionic acid and releases water (29). ^{1}H NMR-spectrum can be found in the supplementary information (Fig. S2). A prominent peak can be observed at $\delta \approx 3.62$ ppm, resulting from the hydrogens in the backbone of the multi-arm molecule. The functional thiol group corresponds to a peak at $\delta \approx 1.65$ ppm, and the two peaks at $\delta \approx 2.65$ and 2.75 ppm correlate to the adjacent methylene groups.

$PEGDMA_{10kDa}$ synthesis – Fig. S1a represents the steps of $PEGDMA_{10kDa}$ synthesis. In this radical polymerization, methacrylic acid and linear PEG_{10kDa} were combined to end-functionalize the molecule. Herein, the PEG hydroxyl end groups would react with the anhydride to form the final structure and methacrylic acid, an unwanted by-product (30). The ^{1}H NMR spectrum (Fig. S3) shows a prominent PEG peak at $\delta \approx 3.64$ ppm, resulting from the hydrogens in the polymer backbone. The methylene protons are typically found at $\delta \approx 5.81$ ppm and $\delta \approx 6.22$ ppm; however, a chemical shift to $\delta \approx 5.56$ ppm and 6.11 ppm can be observed due to deshielding when they connect to PEG. The protons adjacent to the methacrylate groups can be found at $\delta \approx 4.28$ ppm. The methyl groups of the functional group can be found at a chemical shift of $\delta \approx 1.93$ ppm. Small peaks were observed at $\delta \approx 5.29$ and $\delta \approx 1.78$ ppm, which could be assigned as an impurity resulting from the solvent DCM used in the polymer precipitation and water (31). Hence, the product was dried further to remove the solvents.

AlgMA synthesis – The synthesis of alginate methacrylate is represented in Fig. S1c. A

transesterification takes place to allow the addition of the methacryloyl groups of the methacrylic anhydride to the hydroxyl group of the alginate monomer. The ^{1}H NMR spectrum shows that the methylene groups can be found at $\delta \approx 5.66$ ppm and 6.09 ppm, and the methyl resonances at $\delta \approx 1.82$ ppm. The hydrogens in the backbone can be found at $\delta \approx 4.67$ ppm (Fig. S4).

Mechanical characterization of PEGDMA-SH/alginate hydrogels – In this first system, dual network (DN) hydrogels based on $PEGDMA_{10kDa}$-SH (20 wt.%) with alginate (1, 1.5, 2 wt.%) were prepared with calcium sulfate ($CaSO_4$) as a Ca^{2+} crosslinker (5, 10 wt.%) to enable a one-step synthesis of the hydrogels. $CaSO_4$ possesses a low solubility in water and will thus release its calcium ions gradually over time, allowing a direct crosslinking of alginate (32). 3-arm PEG-SH (1:1 ratio with PEGDMA) was added to increase the homogeneity of the network and 0.3 wt.% LAP was incorporated as the photoinitiator. The final structures of the hydrogels were obtained after crosslinking under UV light (254 nm), and all hydrogels were synthesized in triplicates.

The compressive properties of these hydrogels were investigated to determine their mechanical strength. First, samples with variable alginate concentrations were tested using a fixed $CaSO_4$ concentration of 5 wt.% (Fig. 2a). Compared to the single network $PEGDMA_{10kDa}$-SH (SN_{10kDa}) hydrogel, all DN hydrogels showed a significant increase in their Young's Modulus and maximum stress at 90% strain (σ_{max}). Herein, the hydrogel containing 1.5 wt.% alginate achieved the highest compressive strength, closely followed by 1 and 2 wt.%, respectively. Following this, the alginate concentration was set to 1.5 wt.%, and the concentration of $CaSO_4$ increased to 10 wt.% to determine the influence of the Ca^{2+} concentration on the mechanical properties, which showed a significantly increased max. stress compared to the SN_{10kDa} (Fig. 2b). The same trend was observed in hydrogels containing 1 wt.% alginate (Fig. 2c). However, no significant difference in the elastic modulus could be found compared to the DN hydrogels containing 5 wt.% $CaSO_4$ (Fig 2d). Though this system showed increased mechanical properties under compression, the crosslinking of alginate in the presence of $CaSO_4$ happened too abruptly, causing visible segregation within the structure (Fig. S5a, b, black arrows) and making the preparation overly difficult.

To overcome the previously described issue, $CaCO_3$ was employed as a calcium linker to continue a one-pot fabrication of the DN hydrogels with alginate due to the low solubility of this molecule in water. Contrary to $CaSO_4$, $CaCO_3$ does not directly release its Ca^{2+} ions into the environment; instead, it needs to be activated by GDL. The $CaCO_3$ concentrations were based on a paper by Growney Kalaf et al. (33), in which they used a 1:2 $CaCO_3$:GDL ratio and varied the $CaCO_3$ concentrations between 30 and 60 wt.% relative to alginate. Hydrogels were prepared by combining $PEGDMA_{10kDa}$-SH (20 wt.%) with 1 wt.% alginate, crosslinked with $CaCO_3$ and GDL (1:2.5 ratio). While the alginate network crosslinked, it was observed the solution started producing bubbles, which can be correlated to the reaction of $CaCO_3$ with GDL. During calcium release from $CaCO_3$, gluconic acid and CO_2 are produced, which could form bubbles in the hydrogels (34). Hydrogels with a varying concentration of $CaCO_3$ were tested (from 30 to 60 wt.% relative to alginate), demonstrating a direct increase in maximum stress (Fig. 3a). Nevertheless, it is important to mention that the samples exhibited opaqueness (Fig. S5c), suggesting the presence of undissolved $CaCO_3$. Thus, the toughening of the material could be coming from a particle reinforcement instead of the

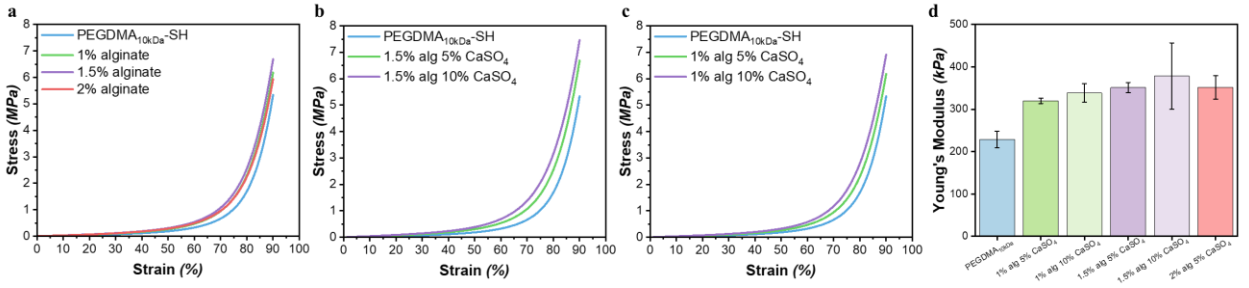

Fig. 2: a-c) Compression testing of $PEGDMA_{10kDa}$/alginate hydrogels with varying alginate and $CaSO_4$ concentrations. d) Young's Modulus of $PEGDMA_{10kDa}$/alginate hydrogels.

incorporation of alginate. Since GDL facilitates the dissolution of $CaCO_3$, we continued to increase this proportion until we achieved transparent hydrogels, which occurred at a $CaCO_3$ to GDL ratio of 1:6.5. The mechanical properties of the hydrogel containing 30 wt.% $CaCO_3$ at this ratio resulted in a decreased σ_{max} compared to a 1:2.5 $CaCO_3$:GDL ratio (Fig. 3b-c), which could suggest that there was indeed particle reinforcement on the previously described formulations. Moreover, the increased GDL content led to an increased bubble formation; thus, we decided to continue with a lower fixed ratio of 1:2.

Next, the concentration of $CaCO_3$ was lowered (10-30 wt.%), and alginate concentrations of 1 and 2 wt.% were used (Fig. S6). Since the ratio with GDL was fixed, the influence of $CaCO_3$ on the opacity, and thus particle reinforcement, could be investigated. The solutions with 1 wt.% alginate and 10 wt.% or 20 wt.% $CaCO_3$ showed no bubble formation, but only the 10 wt.% eliminated all traces of opacity (Fig. S6 vial 1-2). However, this solution required more time to form a gel than the higher $CaCO_3$ concentrations. Increasing the alginate concentration to 2 wt.% resulted in a faster gel formation, producing a clear gel with no bubbles for the formulation consisting of 10 wt.% (Fig. S6 vial 4). Increasing the concentration led to opaque hydrogels with a high presence of bubbles (Fig. S6 vial 5-6).

Despite the relative improvements on the max. stress that was introduced by varying $CaCO_3$ concentration and ratio, it was concluded that the effect was not that significant. According to the literature, the proportion of both networks is important to maximize the results (17). Therefore, we decided to change direction and lowered the PEGDMA-SH content to 15 wt.% (Fig. S5d) and increased the molecular weight to $PEGDMA_{20kDa}$. As could be expected, using $PEGDMA_{20kDa}$-SH impacted the mechanical properties of the material, creating softer hydrogels (Fig. S5e), a behavior that has already been described in the literature (22).

Considering all the above, the mechanical performance of DN hydrogels containing 15 wt.% PEGDMA-SH (10 or 20 kDa) and alginate (1 or 2 wt.%) crosslinked with 10 wt.% $CaCO_3$ in a 1:2 ratio with GDL was tested via compression and tensile testing. Generally, compared to the single network, the incorporation of alginate in the network showed no differences in compressive strength but exhibited increased toughness under elastic forces (Fig 4). Moreover, the Young's Moduli upon compression demonstrated higher values than the ones obtained upon tensile testing (Fig 4 c, f) (15). The networks based on 1 wt.% alginate showed the highest elongation at break of around 300% and 900% for $PEGDMA_{10kDa}$-SH and $PEGDMA_{20kDa}$-SH, respectively, with no increase in Young's Modulus for $PEGDMA_{10kDa}$-SH and a slight increase for $PEGDMA_{20kDa}$-SH (Fig 4b, d). On the other hand, increasing the alginate content to 2 wt.% increased the maximum tensile stress at break (σ_{break}) and Young's Modulus. Hydrogels based on $PEGDMA_{20kDa}$-SH showed lower compressive strength and higher elongation at break than $PEGDMA_{10kDa}$-SH (Fig 4a-b, c-d), which can correlate to higher molar mass segments between crosslinking points, which is in correlation with literature (22, 35).

Thus, DN hydrogels incorporating alginate have shown no differences in compressive strength

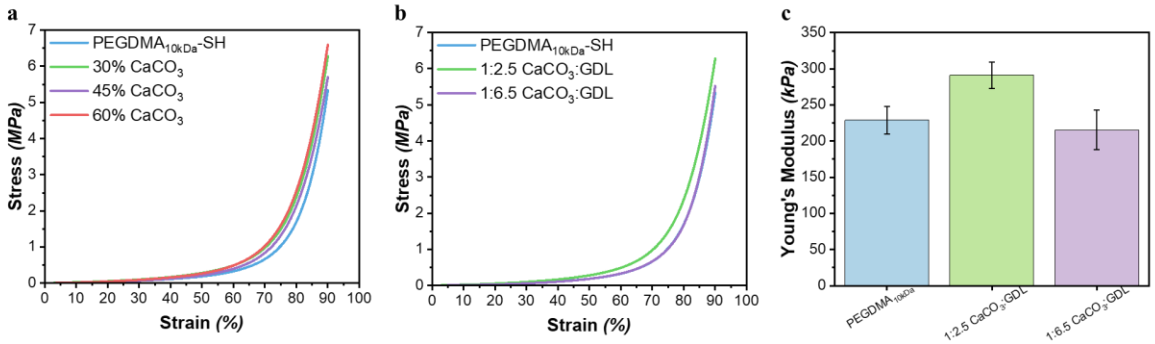

Fig. 3: Characterization of 20 wt.% $PEGDMA_{10kDa}$-SH DN hydrogels. a) Compression results 1 wt.% alginate DN hydrogels with 1:2.5 ratio $CaCO_3$:GDL for increasing $CaCO_3$ concentration; b) DN hydrogels comparing different ratios of $CaCO_3$:GDL containing 30 wt.% $CaCO_3$ and 1 wt.% alginate; c) Young's modulus of compression results in b). Error bars are obtained from standard deviations of triplicates.

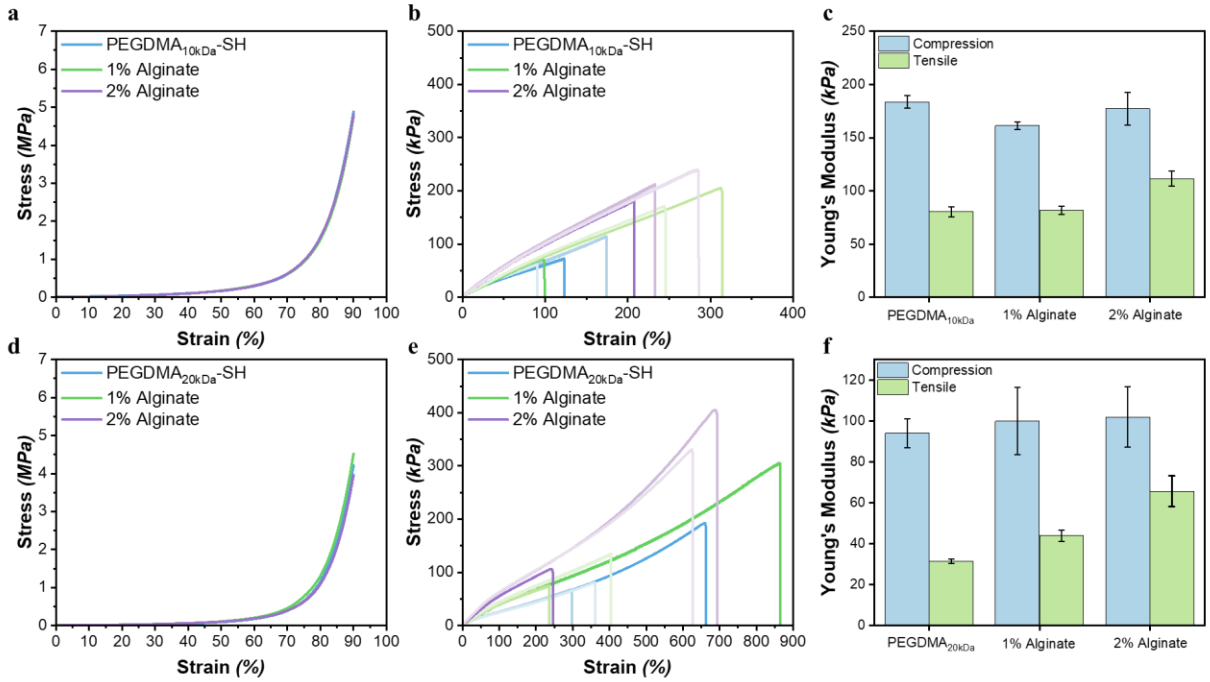

Fig. 4: Comparison of 15 wt.% $PEGDMA_{10kDa}$ and $PEGDMA_{20kDa}$ with different alginate concentrations, crosslinked with 10 wt.% $CaCO_3$ (1:2 ratio with GDL). Mechanical characterization via a, d) compression and b, e) tensile testing. c, f) Representation of Young's Moduli under both mechanical tests for $PEGDMA_{10kDa}$ and $PEGDMA_{20kDa}$. Error bars are obtained from standard deviations of triplicates.

but show increased toughness under tensile compared to the single networks, which was true for both $PEGDMA_{10kDa}$-SH and $PEGDMA_{20kDa}$-SH.

Mechanical characterization of PEGDMA-SH/AlgMA hydrogels – The second system comprised PEGDMA-SH and alginate methacrylate (AlgMA). Linear PEGDMA (MW: 10 or 20 kDa) was combined with AlgMA (1 or 2 wt.%), LAP (0.3 wt.%), $CaCO_3$ (10 wt.%), GDL, and 3-arm PEG-SH (1:1 ratio with MA groups). Alginate methacrylate was included to enable physical (through Ca^{2+}) and chemical crosslinking (via the methacrylate groups), testing the effect of having interconnected networks.

Under compression, both AlgMA concentrations incorporated into the PEGDMA-SH network showed increased max. stress with increasing AlgMA concentrations. Though they showed these improvements, the hydrogels with 2 wt.% AlgMA fractured at approximately 76% and 81% strain for $PEGDMA_{10kDa}$-SH and $PEGDMA_{20kDa}$-SH, respectively (Fig 5a, d). Subsequently, the AlgMA concentration in these hydrogels was reduced to 1.5 wt.%, showing similar behavior to those with 2 wt.% AlgMA by breaking at around 70% strain (Fig S7a). In tensile tests, these hydrogels exhibited an increase in σ_{break} compared to the single network, although the maximum strain decreased for the hydrogels based on $PEGDMA_{20kDa}$-SH (Fig 5b, e). This behavior can be attributed to the increased covalent crosslinking between the MA groups present in both macromonomers, resulting in a higher crosslink density (Table 1). The increased rigidity was particularly evident in the $PEGDMA_{20kDa}$-SH hydrogels, where the strain at break decreased from nearly 700% to 200%. For the lower molecular weight PEGDMA-SH macromonomer, this effect was less pronounced; however, the composition with 2 wt.% AlgMA showed a significant increase in σ_{break} by reaching nearly 1 MPa. Finally, the Young's Modulus of both mechanical tests showed the same consensus, as they increased linearly with AlgMA concentrations (Fig. 5c, f). A similar system created by Wu et al. reported a significant improvement in mechanical properties after introducing PEGDMA to form covalent links between AlgMA and carboxymethyl chitosan, highlighting the importance of covalently connecting polymer networks (36).

The PEGDMA-SH DN hydrogels exhibited significantly increased max. stress under

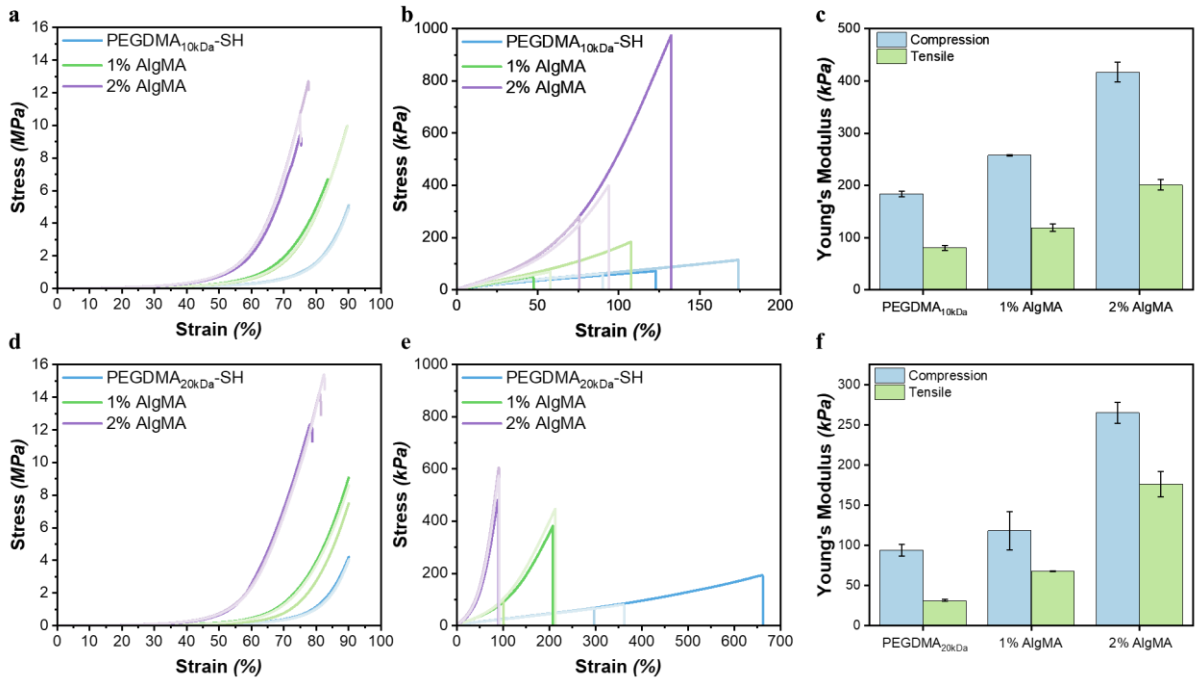

Fig. 5: Comparing the mechanical characteristics of 15 wt.% PEGDMA-SH/AlgMA hydrogels with 1 or 2 wt.% AlgMA crosslinked with 10 wt.% $CaCO_3$ (1:2 ratio with GDL). a, d) Compression results of DN hydrogels based on $PEGDMA_{10kDa}$-SH or $PEGDMA_{20kDa}$-SH. b, e) Results of tensile testing of DN hydrogels. c, f) Elastic modulus of DN hydrogels for compression and tensile results. Error bars are based on the standard deviation of triplicate samples.

compression and tensile for both concentrations of AlgMA compared to the single network and the PEGDMA-SH/alginate DN hydrogels. The highest max stress was achieved by the $PEGDMA_{10kDa}$-SH hydrogels containing 2 wt.% alginate methacrylate. Hydrogels based on $PEGDMA_{20kDa}$-SH showed significantly lowered elongation compared to the single network and the DN hydrogels with alginate. Thus, these results highlight the effects of connecting the two networks on the mechanical properties of the DN hydrogels.

Mechanical characterization of PEGDMA-SH/GelMA hydrogels – DN hydrogels based on PEGDMA-SH with GelMA comprised the third system. To create these hydrogels, 15 wt.% PEGDMA was crosslinked with 3-arm PEG-SH, along with GelMA (2 or 5 wt.%) and LAP (0.3 wt.%). By introducing GelMA into the mixture, the total contribution of MA groups increases, which could influence the mechanical properties due to less structured crosslinking of the hydrogels (22). Hence, the contribution of the SH groups to the mechanical properties of the hydrogels was tested by varying the concentration of 3-arm PEG-SH and evaluating the mechanical performance (Fig. S7b, c). Results from these tests showed that the optimal ratio was a 1:1 thiol to methacrylate group, used previously in synthesizing PEGDMA-SH/alginate and PEGDMA-SH/AlgMA hydrogels.

Compression testing of DN with 2 wt.% GelMA showed an increased σ_{max} for hydrogels made with $PEGDMA_{10kDa}$-SH, but this was not observed for higher molecular weight-based hydrogels (Fig. 6a, d). Furthermore, the elastic modulus showed an increase for both molar mass hydrogels (Fig. 6c, f). The maximum compressive strength increased further when the GelMA concentration was raised to 5 wt.%. Tensile tests revealed that introducing 2 wt.% GelMA to hydrogels consisting of $PEGDMA_{10kDa}$-SH leads to nearly no difference compared to the single network. Increasing the GelMA concentration to 5 wt.% resulted in networks that broke at a much lower max. stress and strain (Fig. 6b). The $PEGDMA_{20kDa}$-SH hydrogels showed significantly reduced elongation, nearly halving that of the single network. However, their σ_{break} remained similar to that of the single network (Fig. 6e).

The increase in brittleness of these networks with increased GelMA concentration can be attributed to the covalent connection between the GelMA and PEGDMA-SH networks, resulting

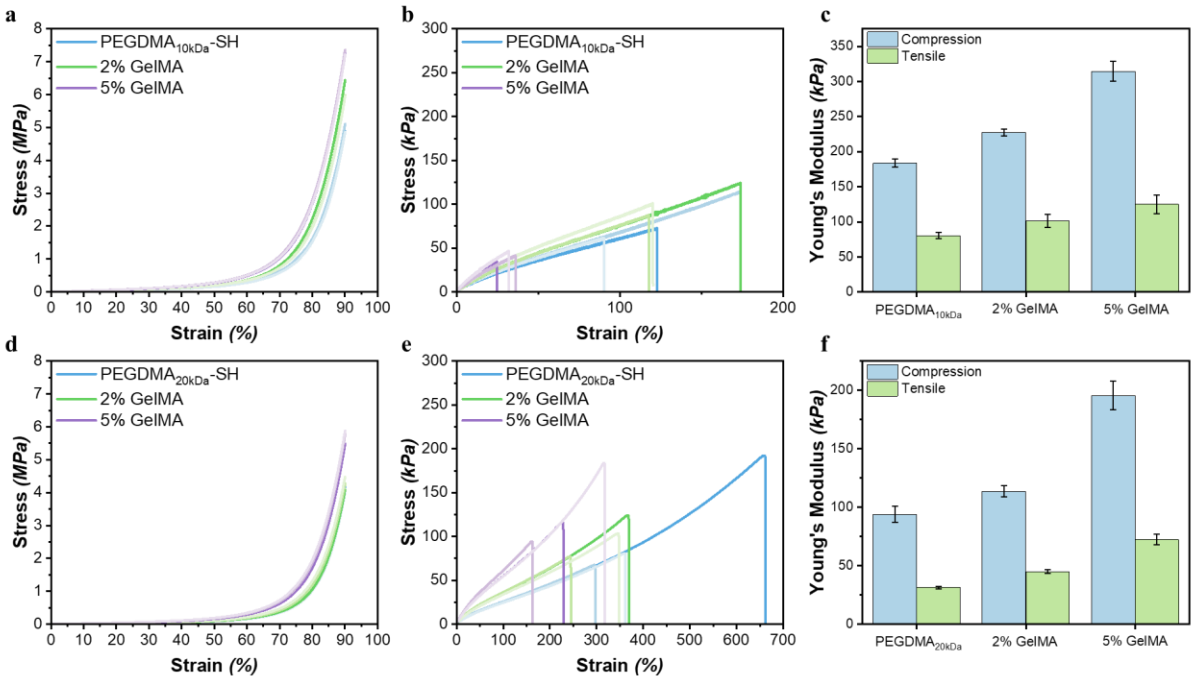

Fig. 6: 15 wt.% PEGDMA-SH/GelMA hydrogels compared by mechanical characteristics. a, d) Compression results for DN hydrogels with 2 and 5 wt.% GelMA compared to the single network. b, e) Characterization based on tensile tests for the SN, 2, and 5 wt.% GelMA. c, f) Comparison of Young's Moduli under compression and tensile testing for $PEGDMA_{10kDa}$-SH and $PEGDMA_{20kDa}$-SH, respectively. Error bars are based on the standard deviation of triplicate samples.

from the presence of MA groups on both macromonomers. The influence of the MA groups was also seen in the dual network hydrogels with AlgMA. However, the PEGDMA-SH/GelMA system showed a greater decrease in stress and a similar decreased elongation at break compared to the AlgMA system.

Swelling testing – Hydrogels for swelling experiments were prepared as previously described. The swelling characteristics were tracked for all hydrogels, excluding the composition with 1 wt.% alginate, as the mechanical properties of this hydrogel resembled those of the 2 wt.% hydrogels. The Flory-Rehner model (See Supporting Information) was used to evaluate the crosslinking density (ρ_c, number of crosslinkers per area) and the mesh size (ζ, average spacing between crosslinks or polymer chains) of the different systems in an aqueous environment. Furthermore, the swelling factor (SF), equilibrium water content (EWC), and gel fraction (GF) were calculated. The SF represents how much a hydrogel can swell when immersed in water, whereas the EWC is correlated with the amount of water that can be retained by a hydrogel when it reaches an equilibrium weight.

Table 1: Swelling factor, equilibrium water content, gel fraction, mesh size, and crosslink density based on the Flory-Rehner model.

Sample	SF (%)	EWC (%)	GF (%)	ζ (nm)	ρ_c (mol/m^{-3})
15 wt.% $PEGDMA_{10kDa}$-SH	256 ± 4	94 ± 0.08	92 ± 3	11 ± 0.08	244 ± 1
$PEGDMA_{10kDa}$-SH/2 wt.% alginate	346 ± 3	95 ± 0.06	88 ± 1	12 ± 0.06	238 ± 1
$PEGDMA_{10kDa}$-SH/1 wt.% AlgMA	211 ± 1	92 ± 0.05	94 ± 1	10 ± 0.04	278 ± 1
$PEGDMA_{10kDa}$-SH/2 wt.% AlgMA	171 ± 4.	90 ± 0.1	93 ± 1	8 ± 0.08	322 ± 3
$PEGDMA_{10kDa}$-SH/2 wt.% GelMA	262 ± 2	94 ± 0.06	95 ± 1	11 ± 0.05	254 ± 1
$PEGDMA_{10kDa}$-SH/5 wt.% GelMA	248 ± 4	92 ± 0.1	98 ± 2	10 ± 0.1	280 ± 3
15 wt.% $PEGDMA_{20kDa}$-SH	370 ± 1	96 ± 0.09	93 ± 1	19 ± 0.2	124 ± 1
$PEGDMA_{20kDa}$-SH/2 wt.% alginate	501 ± 11	97 ± 0.1	79 ± 2	21 ± 0.3	118 ± 1
$PEGDMA_{20kDa}$-SH/1 wt.% AlgMA	260 ± 4	94 ± 0.09	88 ± 1	14 ± 0.1	149 ± 1
$PEGDMA_{20kDa}$-SH/2 wt.% AlgMA	184 ± 3	90 ± 0.1	88 ± 1	11 ± 0.1	207 ± 3
$PEGDMA_{20kDa}$-SH/2 wt.% GelMA	351 ± 6	95 ± 0.1	95 ± 1	17 ± 0.2	133 ± 1
$PEGDMA_{20kDa}$-SH/5 wt.% GelMA	313 ± 4	94 ± 0.09	94 ± 0.3	14 ± 0.1	153 ± 1

SF, swelling factor; **EWC**, equilibrium water content; **GF**, gel fraction; **ζ**, mesh size; **ρ_c**, crosslink density; **PEGDMA**, poly(ethylene glycol) dimethacrylate; **AlgMA**, alginate methacrylate; **GelMA**, gelatine methacrylate.

Lastly, the GF refers to the total percentage of polymer crosslinked to form the hydrogel (Table 1).

For the hydrogels based on $PEGDMA_{10kDa}$-SH, the samples with 2 wt.% alginate achieved the highest SF of 346 ± 3 %, whereas those with 2 wt.% AlgMA showed the lowest value at 171 ± 4 %. A similar trend was observed in the hydrogels based on $PEGDMA_{20kDa}$-SH, in which the highest SF was 501 ± 11 %, and the lowest was 184 ± 3 %, for 2 wt.% alginate and 2 wt.% AlgMA, respectively. Compared to the other systems, the significantly increased SF for the PEGDMA-SH/alginate hydrogels could be correlated to the different crosslinking mechanisms used by the macromonomers, as PEGDMA-SH uses covalent crosslinking. In contrast, alginate uses the Ca^{2+} ions from the environment for crosslinking. Ideally, this would correlate to a more densely crosslinked network; however, the density and the mesh size, as calculated, show the opposite. This could be connected to the physical crosslinking via ionic interactions, which can reverse and diffuse from the network when submerged in water, leading to a less densely crosslinked network over time (13). Moreover, this hydrogel showed a significantly lower GF compared to the other systems, meaning more uncrosslinked material that can diffuse out from the hydrogels during submersion.

All samples demonstrated a high EWC and GF of ≥ 90%, except the $PEGDMA_{10kDa}$-SH/2 wt.% alginate hydrogels and the $PEGDMA_{20kDa}$-SH samples containing alginate and 1 and 2 wt.% AlgMA, of which the GF ranged from 79 % to 88 % (Fig. S7d, e). The highest ρ_c for $PEGDMA_{10kDa}$-SH hydrogels was 322 ± 3 mol/m^{-3}, whereas the lowest was 238 ± 1 mol/m^{-3} for the sample with 2 wt.% AlgMA and 2 wt.% alginate, respectively. A reverse trend was observed for the ζ, in which the highest was reported for the hydrogels with alginate (12 ± 0.06 nm) and the lowest for hydrogels with 2 wt.% AlgMA (8 ± 0.08 nm). Similar trends for ρ_c and ζ are observed for hydrogels based on $PEGDMA_{20kDa}$-SH. In general, hydrogels based on $PEGDMA_{20kDa}$-SH exhibit higher mesh size and lower crosslink density than $PEGDMA_{10kDa}$-SH, which can be correlated with the molecular weight of the polymer. This agrees with what has been reported in the literature by Arreguín-Campos et al. (22) and Haryanto et al. (37).

Overall, the samples based on AlgMA and GelMA exhibited an increased ρ_c compared to the SN hydrogels, which can be correlated to the introduction of MA groups in the second polymer network. These groups are also present in the first network (PEGDMA-SH), which means they can form connections between the two networks rather than within their own network, leading to a higher crosslink density. Moreover, the rigidity increased with the content of the second network in the final structure.

Embedded 3D printing – As mentioned above, the formation of dual networks typically involves difficult preparation protocols, restricting their processability. Arguably, among the different systems that we have described, the one comprising alginate would be the most challenging to process. Thus, as a proof-of-concept, we selected a specific composition for embedded 3D printing (Fig. 7a), an extrusion-based technique where the structure is printed in a support bath that is later removed (38, 39). The selected composition included $PEGDMA_{10kDa}$-SH and 2 wt.% alginate due to its

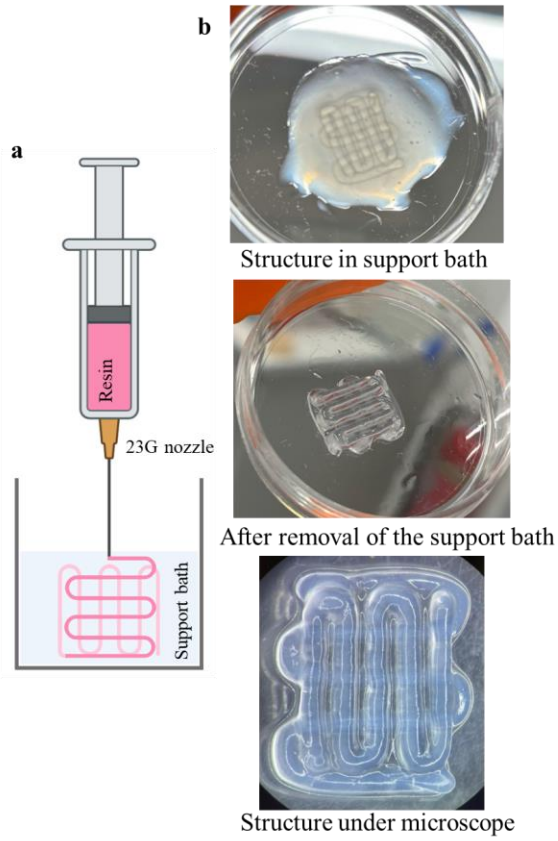

Fig. 7: Embedded 3D printing results. a) Schematic representation of embedded 3D printing. b) The printed two-layered structure in the support bath, when the support bath was removed, and lastly, viewed with a microscope (from top to bottom).

favorable viscosity and elastic properties, enabling physical and chemical crosslinking. The support bath was washed with $CaCl_2$ before use, which incorporated Ca^{2+} ions into the structure for alginate crosslinking (removing the need to add $CaCO_3$ and GDL), while PEGDMA-SH was crosslinked with UV irradiation every two layers for 30 seconds. The nozzle size was found to significantly impact layer printing; 23G (diameter = 0.33 mm) provided the best results, whereas 22G (diameter = 0.41 mm) and 25G (diameter = 0.25 mm) nozzles led to distorted structures and more frequent clogging (Fig. S8b). Another aspect to consider is the opacity of the support bath, which can contribute to insufficient penetration of UV light into the structure, inevitably lowering the resolution of the printed structure.

This technique allowed us to print a 3D structure comprising two separate layers, of which the strand thickness was 1 mm. This demonstrates the possibility of our system being processed via this technique, as well as the potential for patient-tailored applications of these types of biomaterials (Fig. 7b).

Cell viability testing –The hydrogels described here must be non-toxic when used as replacements for load-bearing tissues within the body. First, 15

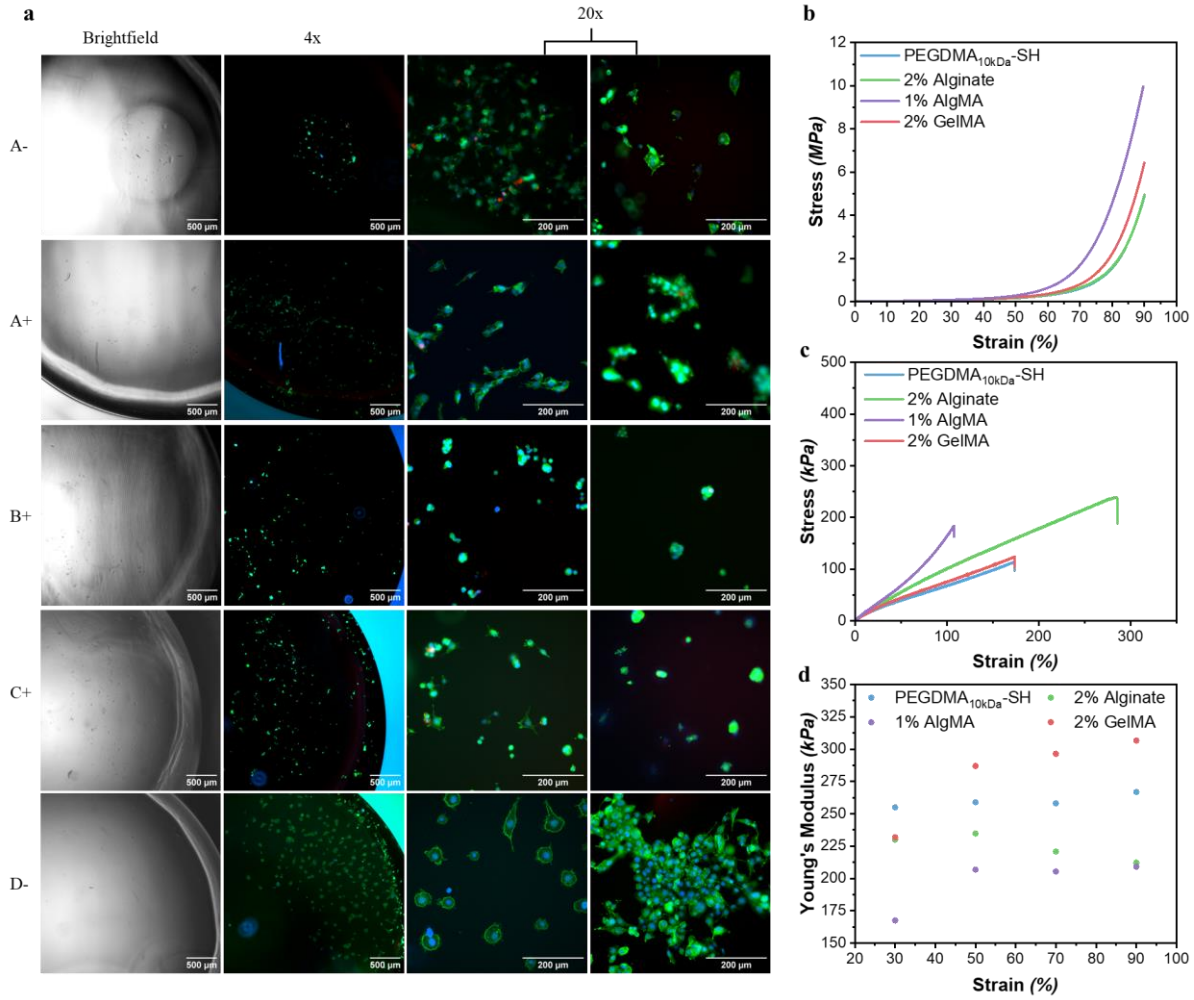

Fig. 8: a) Day one live/dead assay of 15 wt.% $PEGDMA_{10kDa}$-SH SN hydrogels without RGD (A-), SN with RGD (A+), PEGDMA-SH/alginate (2 wt.%) hydrogels with RGD (B+), DN hydrogels with PEGDMA-SH, AlgMA (1 wt.%) and RGD (C+), and PEGDMA-SH/GelMA (2 wt.%) DN hydrogels without RGD (D-). The first column shows the brightfield view under the microscope, highlighting the edge of the hydrogels at 4x magnification. The second column presents fluorescent images of the same location and magnification. The last two columns display fluorescent imaging of cells at a higher magnification of 20x. Scale bars are 500 µm and 200 µm for the first and last two columns, respectively. The nuclei are colored with DAPI (blue), and F-actin is stained with phalloidin (green). b) Comparison of compression results of the selected hydrogels used in cell testing. c) Tensile testing comparison between the different hydrogels used for cell experiments. d) Comparison of the Young's Moduli under cyclic compression for the hydrogels.

wt.% SN_{10kDa} hydrogels with (A+) and without (A-) RGD were selected to establish a baseline of viability. Next, we selected compositions based on 15 wt.% $PEGDMA_{10kDa}$-SH/2 wt.% alginate (B+), $PEGDMA_{10kDa}$-SH/1 wt.% AlgMA (C+), and $PEGDMA_{10kDa}$-SH/2 wt.% GelMA (D-). The alginate and AlgMA hydrogels were enriched with RGD to facilitate cell adhesion, whereas GelMA inherently contains the domains required for cell adhesion (13, 40). ATDC5 cells (15.000 cells/well) were cultured for 24 hours on the selected hydrogels to investigate the biocompatibility. These cells were chosen because they are chondrogenic, similar to chondrocytes, which are responsible for cartilage deposition (41). Generally, all samples demonstrated good biocompatibility, with very few dead cells on the hydrogels (Fig. 8a). Brightfield images show the edge of the hydrogels, and the second column shows the cells in the same location and magnification. The last two columns show cells from this location in a higher magnification of 20x.

The A- hydrogels, not enriched with RGD, caused most cells to migrate from the hydrogel to the sides of the well; however, in the first row, we observed a bubble in the hydrogel that did retain cells. At 20x magnification, few dead cells were noted. The A+ hydrogels showed more cell attachment due to the presence of RGD, with cells exhibiting elongated actin fibers related to relaxed cells. Hydrogels B+ and C+ also showed good biocompatibility and cell clustering on the hydrogels. Under higher magnification, cells on hydrogels C+ displayed more relaxation (elongated actin fibers) compared to B+ hydrogels. Finally, cells on D- hydrogels migrated less prominently to the sides of the gel, showed very few dead cells, and nicely elongated actin fibers, even when clustered. Additionally, the last image in this row shows cells in multiple planes, indicating cell migration into the hydrogel. Though all hydrogels exhibit low numbers of dead cells, the cells showed the most relaxed characteristics (elongation of actin fibers) when seeded on hydrogels containing GelMA (D-).

Comparison between systems – Based on the compositions used for cell viability testing, we compared the mechanical performance of the different systems (Fig 8b-d). Generally, interconnecting the networks via methacrylate groups resulted in increased compressive strength, while the system without this connection did not show an increased strength. Additionally, reinforcing this covalent connection with physical crosslinking in the system with AlgMA enhanced the performance of the hydrogels even further (Fig. 8b). On the other hand, the DN hydrogel with alginate showed the highest elongation and stress at break under tensile conditions, whereas the hydrogels with GelMA showed similar results to the single network. The dual networks with PEGDMA-SH and AlgMA showed the lowest strain at break (Fig. 8c).

Stepwise cyclic compression was performed on the same compositions to investigate the energy dissipation mechanism (Fig. 8d, Fig. S9). Overall, Young's Moduli for all samples remained relatively consistent, with a small increase with each step, likely due to the samples drying out. This resulted in an increase in total polymer content, thereby raising the elastic modulus, as Arreguín-Campos et al. reported (21). The only exception was observed in the samples based on $PEGDMA_{10kDa}$-SH/alginate, where the modulus decreased with increased strain. This decrease could be attributed to breaking the chains, which overpowered the dehydration effect seen in the other systems.

Considering all the above, introducing the type of second network into the PEGDMA-SH matrix allows the tunability of different properties of the hydrogels and can facilitate processing. For example, the incorporation of GelMA (D-) does not improve the mechanical properties of the hydrogel enormously; however, it introduces cell attachment sites, showing improved attachment compared to the single network with RGD (A+).

CONCLUSION

Improving the mechanical properties of hydrogels is crucial for their application as load-bearing tissue replacements, such as cartilage and bone. Different crosslinking mechanisms for various macromonomers enable a one-step synthesis, facilitating patient-specific applications.

This study synthesized three different systems by incorporating alginate, alginate methacrylate, and gelatine methacrylate into a PEGDMA-SH network. While the incorporation of alginate did not exhibit any improved compressive properties, it demonstrated increased toughness under tensile conditions due to the possible energy dissipation mechanism provided by alginate. Contrary to our expectations, the crosslink density and mesh size

were lower despite introducing a second network. On the other hand, providing covalent crosslinking between the two networks increased the compressive strength, as seen in the dual networks with AlgMA and GelMA. The increase in max. stress was more prominent in the AlgMA network. However, both systems showed similar or decreased elongation under elastic forces, which can be correlated to the increased crosslink density and mesh size. All three systems exhibit good biocompatibility after 24 hours with ADTC5 cells. However, the dual network incorporating GelMA showed the most attached cells on the hydrogel with nicely elongated actin fibers. Furthermore, we demonstrate the printability of the system by incorporating alginate via embedded 3D printing and successfully printing a two-layered structure. This same strategy could be extended to the AlgMA system.

Our findings demonstrate that introducing a second network to the PEGDMA-SH matrix enhances mechanical properties. Using different crosslinking mechanisms tailored to the specific network allows for tunable properties and supports the processing of hydrogels for patient-tailored applications.

REFERENCES

1. Mhanna R, Hasan A. Introduction to Tissue Engineering: Regenerative Medicine, Smart Diagnostics and Personalized Medicine. 2017. p. 1-34.
2. Killion JA, Geever LM, Devine DM, Kennedy JE, Higginbotham CL. Mechanical properties and thermal behaviour of PEGDMA hydrogels for potential bone regeneration application. Journal of the Mechanical Behavior of Biomedical Materials. 2011;4(7):1219-27.
3. Black CR, Goriainov V, Gibbs D, Kanczler J, Tare RS, Oreffo RO. Bone Tissue Engineering. Curr Mol Biol Rep. 2015;1(3):132-40.
4. Kneser U, Schaefer DJ, Munder B, Klemt C, Andree C, Stark GB. Tissue engineering of bone. Minimally Invasive Therapy & Allied Technologies. 2002;11(3):107-16.
5. Chan BP, Leong KW. Scaffolding in tissue engineering: general approaches and tissue-specific considerations. Eur Spine J. 2008;17 Suppl 4(Suppl 4):467-79.
6. Liu C, Xia Z, Czernuszka JT. Design and Development of Three-Dimensional Scaffolds for Tissue Engineering. Chemical Engineering Research and Design. 2007;85(7):1051-64.
7. Dhandayuthapani B, Yoshida Y, Maekawa T, Kumar DS. Polymeric Scaffolds in Tissue Engineering Application: A Review. International Journal of Polymer Science. 2011;2011:290602.
8. D'Amora U, Ronca A, Raucci MG, Ambrosio L. Chapter 6 - Overview of scaffolds processing technologies. In: Boccaccini AR, Ma PX, Liverani L, editors. Tissue Engineering Using Ceramics and Polymers (Third Edition): Woodhead Publishing; 2022. p. 215-62.
9. Spiller KL, Maher SA, Lowman AM. Hydrogels for the repair of articular cartilage defects. Tissue Eng Part B Rev. 2011;17(4):281-99.
10. Ahmed EM. Hydrogel: Preparation, characterization, and applications: A review. Journal of Advanced Research. 2015;6(2):105-21.
11. Kopeček J, Yang J. Hydrogels as smart biomaterials. Polymer International. 2007;56(9):1078-98.
12. Yahia L. History and Applications of Hydrogels. Biomedical Sciences. 2015;04(02).
13. Lee KY, Mooney DJ. Hydrogels for Tissue Engineering. Chemical Reviews. 2001;101(7):1869-80.
14. Zhu J. Bioactive modification of poly(ethylene glycol) hydrogels for tissue engineering. Biomaterials. 2010;31(17):4639-56.
15. Burke G, Cao Z, Devine DM, Major I. Preparation of Biodegradable Polyethylene Glycol Dimethacrylate Hydrogels via Thiol-ene Chemistry. Polymers. 2019;11(8):1339.
16. Zhang W, Chen S, Jiang W, Zhang Q, Liu N, Wang Z, et al. Double-network

hydrogels for biomaterials: Structure-property relationships and drug delivery. European Polymer Journal. 2023;185:111807.
17. Gong JP. Why are double network hydrogels so tough? Soft Matter. 2010;6(12):2583-90.
18. Xin H. Double-Network Tough Hydrogels: A Brief Review on Achievements and Challenges. Gels. 2022;8(4):247.
19. Gyles DA, Castro LD, Silva JOC, Ribeiro-Costa RM. A review of the designs and prominent biomedical advances of natural and synthetic hydrogel formulations. European Polymer Journal. 2017;88:373-92.
20. Lopes J, Fonseca R, Viana T, Fernandes C, Morouço P, Moura C, et al. Characterization of Biocompatible Poly(Ethylene Glycol)-Dimethacrylate Hydrogels for Tissue Engineering. Applied Mechanics and Materials. 2019;890:290-300.
21. Arcaute K, Mann BK, Wicker RB. Stereolithography of Three-Dimensional Bioactive Poly(Ethylene Glycol) Constructs with Encapsulated Cells. Annals of Biomedical Engineering. 2006;34(9):1429-41.
22. Arreguín-Campos M, Ebrahimi M, Dookhith AZ, Lynd NA, Sanoja GE, Aldana AA, et al. Architectural differences in photopolymerized PEG-based thiol-acrylate hydrogels enable enhanced mechanical properties and 3D printability. European Polymer Journal. 2024;212:113070.
23. Creton C. 50th Anniversary Perspective: Networks and Gels: Soft but Dynamic and Tough. Macromolecules. 2017;50(21):8297-316.
24. Ishikawa S, Sakai T. One-Pot Approach to Synthesize Tough and Cell Adhesive Double-Network Hydrogels Consisting of Fully Synthetic Materials of Self-Assembling Peptide and Poly(ethylene glycol). ACS Applied Bio Materials. 2023;6(12):5282-9.
25. Yuan Y, Tyson C, Szyniec A, Agro S, Tavakol TN, Harmon A, et al. Bioactive Polyurethane–Poly(ethylene Glycol) Diacrylate Hydrogels for Applications in Tissue Engineering. Gels. 2024;10(2):108.
26. Chen Q, Chen H, Zhu L, Zheng J. Fundamentals of double network hydrogels. Journal of Materials Chemistry B. 2015;3(18):3654-76.
27. Kopeček J. Hydrogel biomaterials: A smart future? Biomaterials. 2007;28(34):5185-92.
28. Sun J-Y, Zhao X, Illeperuma WRK, Chaudhuri O, Oh KH, Mooney DJ, et al. Highly stretchable and tough hydrogels. Nature. 2012;489(7414):133-6.
29. Mulay P, Shrikhande G, Puskas JE. Synthesis of Mono- and Dithiols of Tetraethylene Glycol and Poly(ethylene glycol)s via Enzyme Catalysis. Catalysts. 2019;9(3):228.
30. Lin-Gibson S, Bencherif S, Cooper JA, Wetzel SJ, Antonucci JM, Vogel BM, et al. Synthesis and Characterization of PEG Dimethacrylates and Their Hydrogels. Biomacromolecules. 2004;5(4):1280-7.
31. Fulmer G, Miller A, Sherden N, Gottlieb H, Nudelman A, Stoltz B, et al. NMR Chemical Shifts of Trace Impurities: Common Laboratory Solvents, Organics, and Gases in Deuterated Solvents Relevant to the Organometallic Chemist. Organometallics. 2010;29.
32. Stewart M, Arnold K. Chapter 3 - Produced Water Treating Systems. In: Stewart M, Arnold K, editors. Emulsions and Oil Treating Equipment. Burlington: Gulf Professional Publishing; 2009. p. 107-211.
33. Growney Kalaf EA, Flores R, Bledsoe JG, Sell SA. Characterization of slow-gelling alginate hydrogels for intervertebral disc tissue-engineering applications. Materials Science and Engineering: C. 2016;63:198-210.
34. Maxwell C, Soltisz A, Rich W, Choi A, Reilly M, Swindle-Reilly K. Alginate Hydrogels as Injectable Drug Delivery Vehicles for Optic Neuropathy Treatment2021.
35. Macdougall LJ, Truong VX, Dove AP. Efficient In Situ Nucleophilic Thiol-yne Click

Chemistry for the Synthesis of Strong Hydrogel Materials with Tunable Properties. ACS Macro Letters. 2017;6(2):93-7.
36. Wu P, Fang Y, Chen K, Wu M, Zhang W, Wang S, et al. Study of double network hydrogels based on sodium methacrylate alginate and carboxymethyl chitosan. European Polymer Journal. 2023;194:112137.
37. Haryanto, Kim S, Kim J, Kim J, Ku S, Cho H, et al. Fabrication of poly(ethylene oxide) hydrogels for wound dressing application using E-beam. Macromolecular Research. 2014;22.
38. Budharaju H, Sundaramurthi D, Sethuraman S. Embedded 3D bioprinting – An emerging strategy to fabricate biomimetic & large vascularized tissue constructs. Bioactive Materials. 2024;32:356-84.
39. Kajtez J, Wesseler MF, Birtele M, Khorasgani FR, Rylander Ottosson D, Heiskanen A, et al. Embedded 3D Printing in Self-Healing Annealable Composites for Precise Patterning of Functionally Mature Human Neural Constructs. Advanced Science. 2022;9(25):2201392.
40. Davidenko N, Schuster CF, Bax DV, Farndale RW, Hamaia S, Best SM, et al. Evaluation of cell binding to collagen and gelatin: a study of the effect of 2D and 3D architecture and surface chemistry. J Mater Sci Mater Med. 2016;27(10):148.
41. Yao Y, Wang Y. ATDC5: an excellent in vitro model cell line for skeletal development. J Cell Biochem. 2013;114(6):1223-9.

Acknowledgements – Jacobs A. extends heartfelt gratitude to Arreguín-Campos M. for her guidance during the internship. The author also expresses sincere thanks to Prof. Dr. Pitet L. for the opportunity to join his Advanced Functional Polymers (AFP) research group for her internship. Jacobs A. would like to thank the other group members for the pleasant work environment and their help and insights when needed. Furthermore, she would like to thank Prof. Dr. Baker M. for providing the cell testing facilities and Beeren I. for supporting the cell viability testing. Finally, she would like to thank her parents, family, and friends for their unconditional support during the internship, especially during the hardships.

Author contributions – Pitet. L. and Arreguín-Campos M. designed and supervised the project. Jacobs A. and Arreguín-Campos M. performed laboratory tasks and methodology. Jacobs A. wrote and reviewed the manuscript and performed data analysis. Arreguín-Campos M. helped analyze the data and guided and supervised the project. All authors were responsible for carefully reviewing and editing the manuscript.

SUPPORTING INFORMATION

NMR spectroscopy – A JEOL spectrometer operating at room temperature with a frequency of 400 MHz retrieved the NMR spectra of the synthesized polymers. PEGDMA samples were dissolved in $CDCl_3$, while alginate/AlgMA samples were dissolved in D_2O. Both had a final concentration of approximately 10 mg/mL. All chemical shifts (δ) are reported in parts per million (ppm) relative to the chemical shift of the solvent ($CDCl_3$, ^1H δ = 7.26 ppm; D_2O, ^1H δ = 4.80 ppm).

Hydrogels with varying thiol ratios – $PEGDMA_{10kDa}$/GelMA hydrogels were prepared, in which the 3-arm PEG-SH ratios were varied. 3-arm PEG-SH and LAP were dissolved in water, after which this solution was added to $PEGDMA_{10kDa}$; GelMA was dissolved separately. After this, the PEGDMA-SH mixture was added to GelMA and vortexed until combined. The solution was pipetted into the molds for mechanical testing and crosslinked under UV light for 15 minutes.

Calculations related to the swelling experiments - To calculate the gel fraction (GF%), the gels were weighed directly after removing them from the mold (W_0) and placed in a vacuum oven to dry overnight to record the dry weight (W_d). These measurements were done for gels synthesized with and without crosslinker and in triplicates.

$$GF\ (\%) = \frac{W_d}{W_0}\ x\ 100\ \%$$

Then, the equilibrium water content (EWC) was calculated by measuring the weight after reaching an equilibrium in water (W_1). Afterward, the gels were dried in the vacuum oven, and their weight was re-recorded (W_{dd}).

$$ECW\ (\%) = \frac{W_1 - W_{dd}}{W_1}\ x\ 100\ \%$$

And the swelling factor (SF) was determined as follows:

$$SF\ (\%) = \frac{W_t}{W_0}\ x\ 100\%$$

where W_t is the final measured weight before drying, and W_0 is the initial wet weight before immersed.

The mesh size and crosslink density of the hydrogel were calculated through the Flory-Rehner calculations, where first, the swelling ratio based on the hydrogel mass (Q_M) was calculated:

$$Q_M = \frac{M_s}{M_d}$$

where M_s is the hydrogel mass after swelling and M_d the mass of the dry hydrogel.

Using this Q_M, the volume swelling ratio (Q_v) was expressed as:

$$Q_V = 1 + \frac{\rho_p}{\rho_s}\ x\ (Q_M - 1)$$

where ρ_p is the density of the hydrogel (1.13 g/cm³) and ρ_s the density of the solvent (1 g/cm³).

Then, the molecular weight between the cross-linking points (M_c) was calculated as follows:

$$\frac{1}{\bar{M}_C} = \frac{2}{\bar{M}_n} - \frac{\frac{\bar{v}}{V_1}(\ln(1 - v_2) + v_2 + \chi_1 v_2^2)}{v_2^{1/3} - \frac{v_2}{2}}$$

where $\bar{M}_n$ is the number-average molecular weight of the un-crosslinked hydrogel, V_1 is the molar volume of water (18 cm³), v_2 is the polymer volume fraction in the swollen hydrogel at equilibrium

($1/Q_v$), $\bar{\upsilon}$ is the specific volume of the polymer ($1/\rho_p$), and χ_1 is the parameter for the polymer-solvent interaction (0.246 for PEG-H_2O).

Subsequently, the root-mean-square end-to-end distance of the polymer chain in the unperturbed state ($(\bar{r}_0^2)^{\frac{1}{2}}$) was calculated:

$$\left((\bar{r}_0^2)^{\frac{1}{2}}\right) = lC_n^{1/2}n^{1/2}$$

Where l is the average bond length (0.146 nm), C_n is the characteristic ratio of the polymer (4.0 for PEG), and n is the number of bonds in the cross-link where n equals:

$$n = 2\frac{\bar{M}_c}{M_r}$$

Where M_r is the molecular weight of the repeat unit (44 for PEG).

Finally, the mesh size was calculated as follows:

$$\zeta = v_2^{-1/3}(\bar{r}_0^2)^{1/2}$$

Based on these results, the crosslink density was calculated:

$$\rho_p = \frac{1}{\bar{\upsilon}\,\bar{M}_c}$$

Support bath synthesis – A support bath based on gelatine and Arabic gum was created as described elsewhere. Before use, the support bath was centrifuged for 5 minutes at 800g. The supernatant was drained, replaced by $CaCl_2$ (125 mM), and centrifuged at 1000g for 5 minutes. The same steps were repeated two more times. After this, a final centrifugation took place at 2000g for 10 minutes, after which the supernatant was drained, and the bath was left for one hour before printing. The washing takes place with $CaCl_2$ to allow the incorporation of calcium ions into the bath to facilitate alginate crosslinking.

DAPI/Phalloidin staining of cells – Cells were initially fixed with a formaldehyde solution and washed three times with PBS. Following this, the PBS was removed and replaced with Triton X (0.1% in PBS), which was left for 30 minutes before being removed and washed three times with PBS. Subsequently, a blocking solution containing 3% bovine serum albumin was added and left for one hour. The gels were then washed twice with PBS. Next, a solution of DAPI (1:300) and phalloidin 488 (1:100) in the blocking solution was added and left for one hour, followed by three final washes of PBS. Imaging was performed the next day.

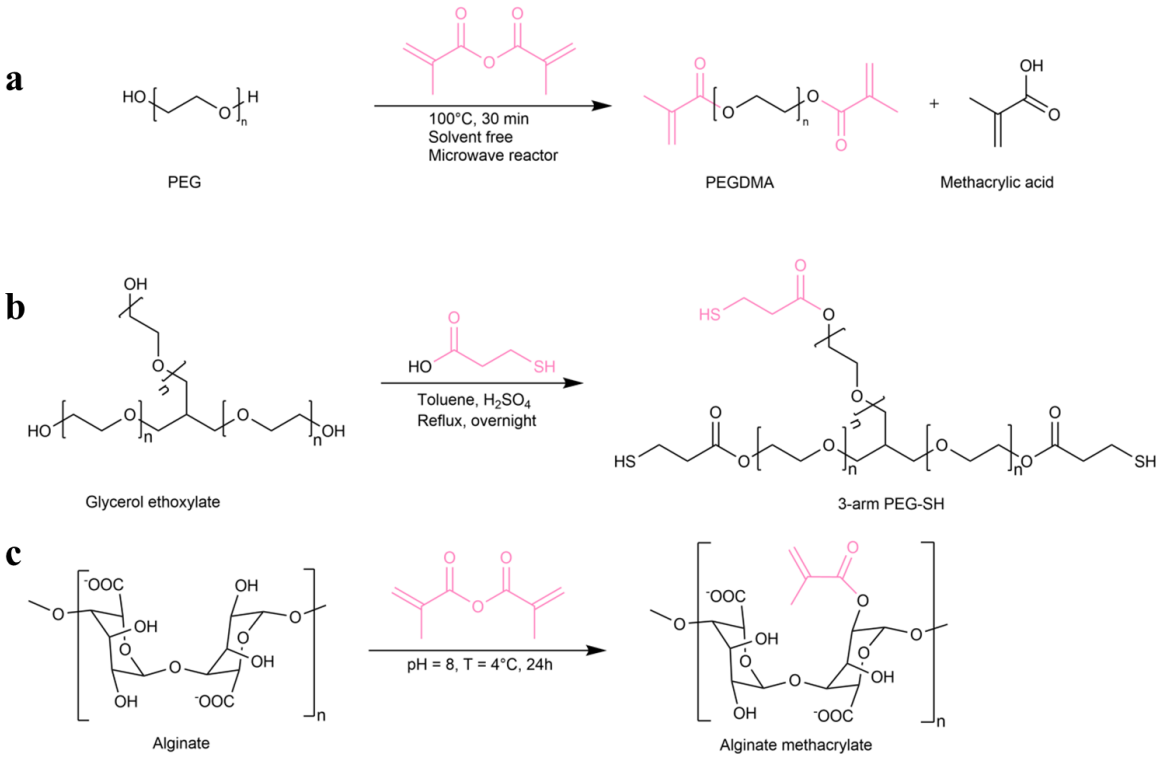

Fig. S1: Reaction schemes of a) PEGDMA, b) 3-arm PEG-SH, and c) alginate methacrylate synthesis.

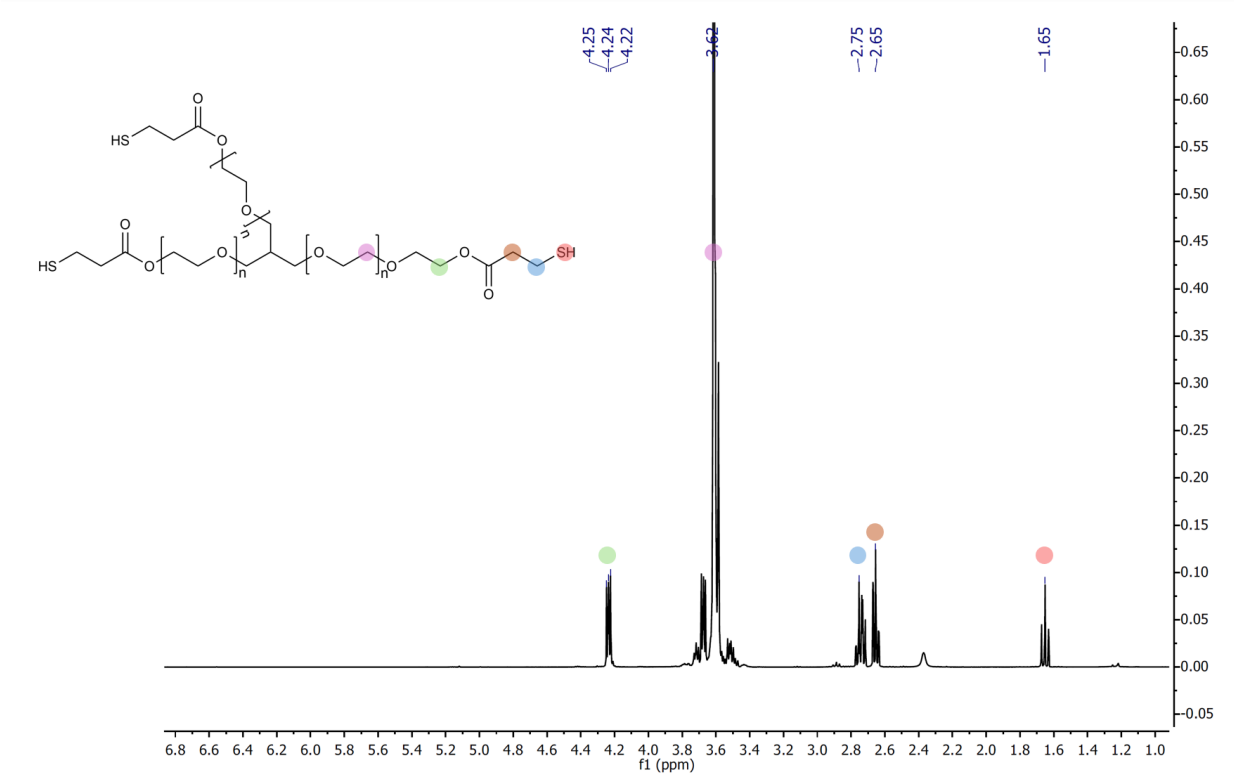

Fig. S2: ^{1}H NMR spectrum of 3-arm PEG-SH in $CDCl_3$ (400 MHz).

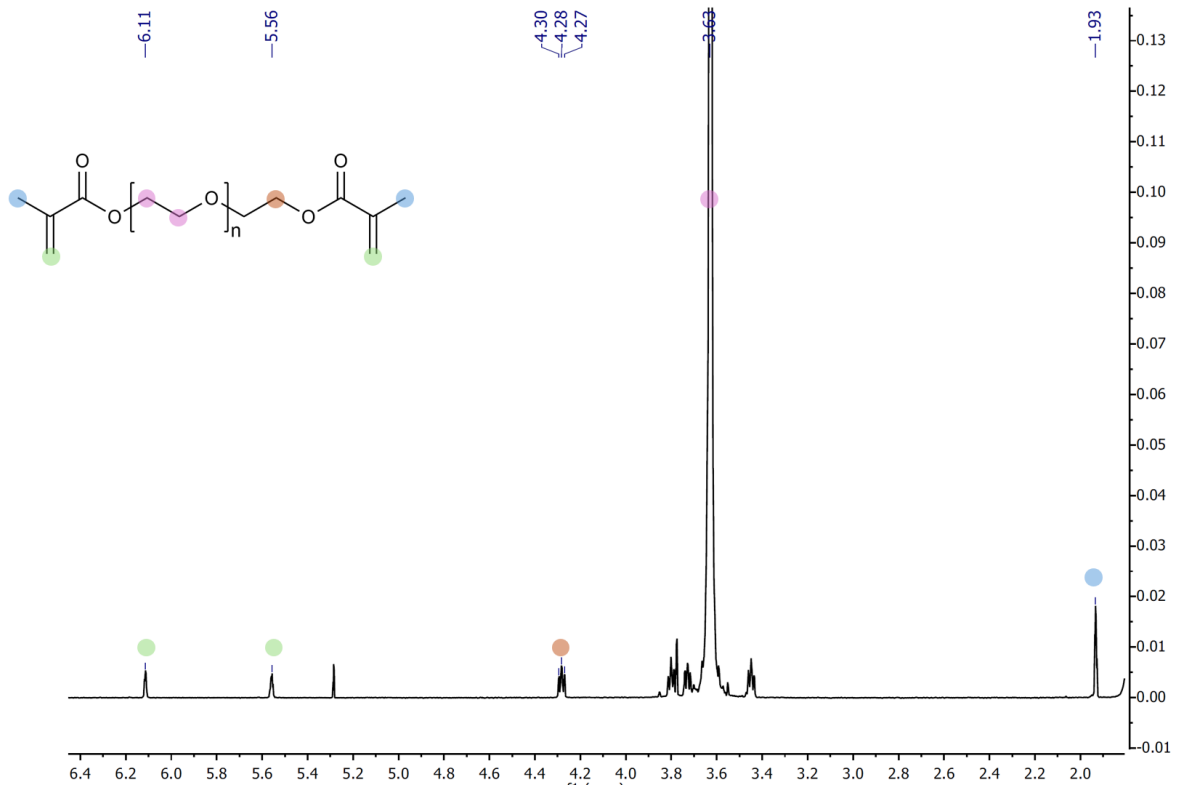

Fig. S3: ^{1}H NMR spectrum of poly(ethylene glycol) modified with methacrylic anhydride in deuterated chloroform at 400 MHz.

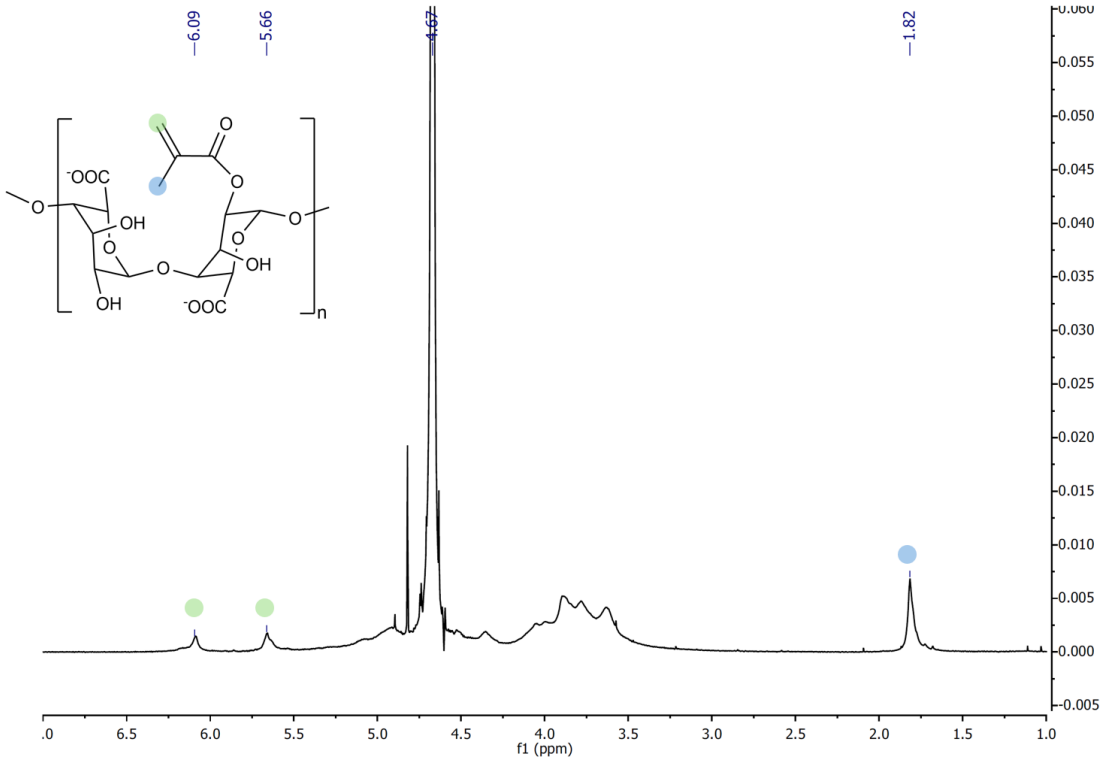

Fig. S4: alginate modified with methacrylic anhydride ^{1}H NMR spectrum ($CDCl_3$, 400 MHz).

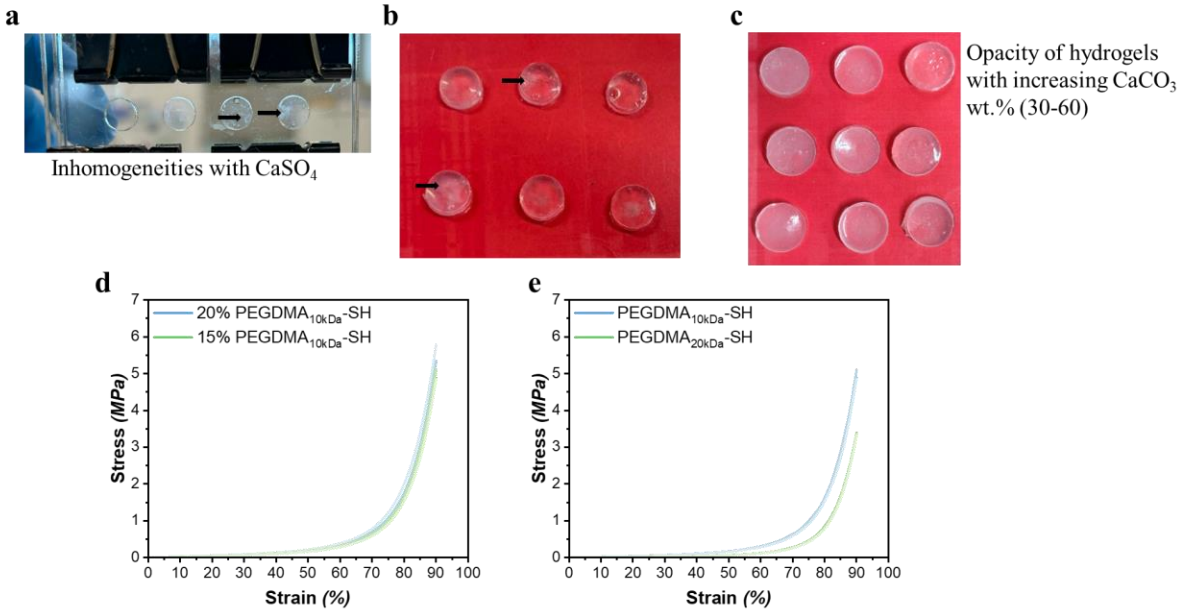

Fig. S5: a, b) inhomogeneity of the PEGDMA-SH/alginate hydrogel when crosslinked with $CaSO_4$. c) opacity of the alginate DN hydrogels with 30-60 wt.% $CaCO_3$ (top: 30%, middle: 45%, bottom: 60%). d) comparison of 20 wt.% and 15 wt.% $PEGDMA_{10kDa}$-SH. e) Comparing $PEGDMA_{10kDa}$-SH and $PEGDMA_{20kDa}$-SH.

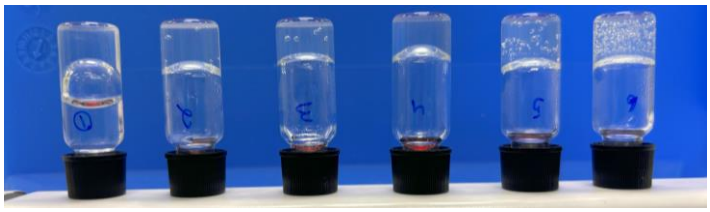

Fig. S6: Crosslinking of alginate (1 and 2 wt.%) with different $CaCO_3$ concentrations in a 1:2 ratio with GDL. 1-3) 1 wt.% alginate with 10, 20, and 30 wt.% $CaCO_3$, respectively; 4-6) 2 wt.% alginate with 10-30 wt.% $CaCO_3$. Vials 5 and 6 show prominent bubble formation, which is minimal in vials 2 and 3. Bubble formation is not present in vials 1 and 4.

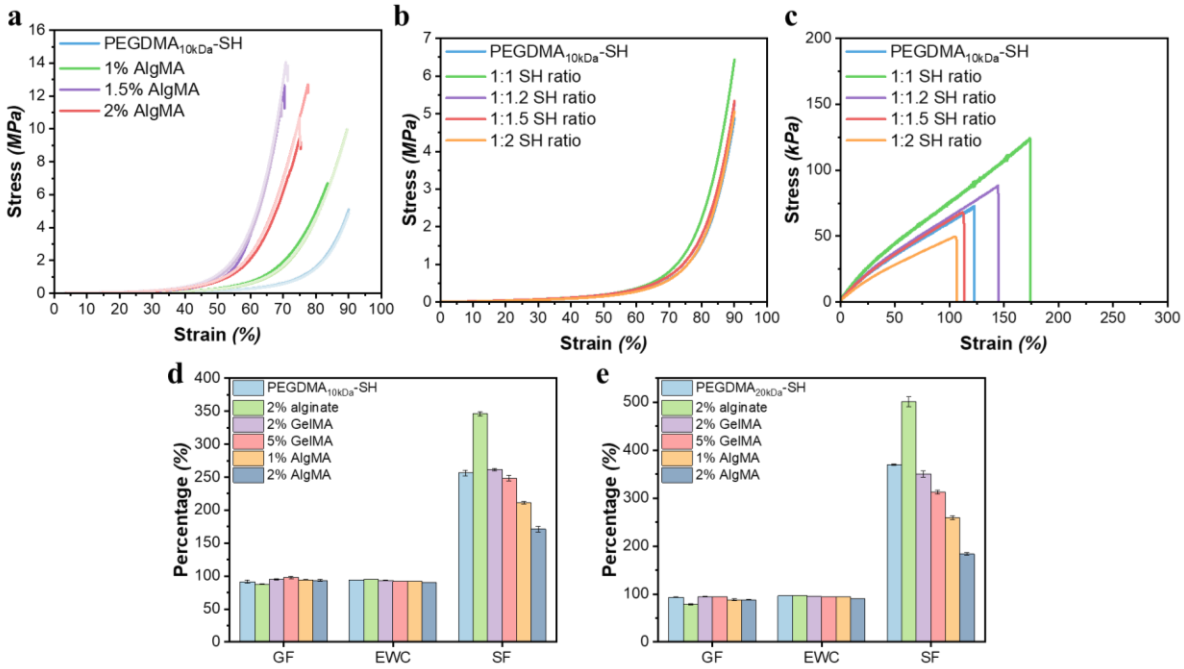

Fig. S7: Mechanical characterization of methacrylate functionalized hydrogels. a) AlgMA hydrogels with 1, 1.5, and 2 wt.%. b) Compression results of PEGDMA-SH/GelMA hydrogels with different thiol concentrations. c) Tensile testing of different thiol concentrations for GelMA DN hydrogels. d, e) Results of swelling experiments for PEGDMA-SH of MW 10kDa and 20kDa.

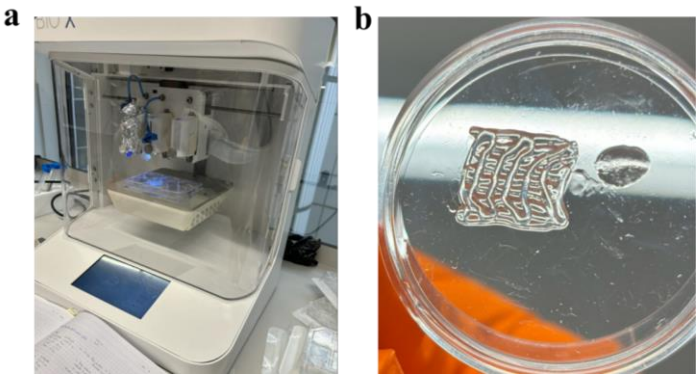

Fig. S8: Embedded 3D printing. a) BioX bioprinter. b) Distorted two-layered structure printed with embedded 3D printing.

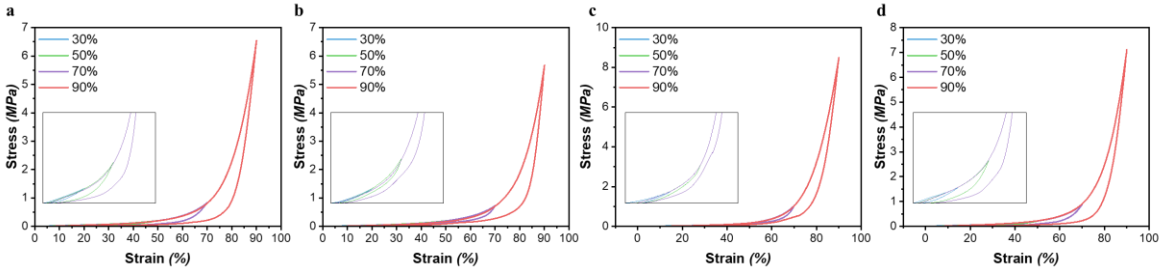

Fig. S9: Cyclic compression of a) 15 wt.% SN PEGDMA$_{10kDa}$-SH hydrogels, b) DN hydrogels with 2 wt.% alginate, c) PEGDMA$_{10kDa}$-SH/1 wt.% AlgMA hydrogels, and d) DN hydrogels with GelMA.